OAK RIDGE NATIONAL LABORATORY

MANAGED BY UT-BATTELLE, LLC.
POST OFFICE BOX 2008, OAK RIDGE, TENNESSEE 37831-6079

ORNL
CENTRAL FILES NUMBER

ORNL/CF-00/34

DATE: November 13, 2000

SUBJECT: Quarterly Technical Progress Report of the Radioisotope Power System Materials Production and Technology Program Tasks for July through September 2000

TO: Distribution

FROM: J. P. Moore J.P. Moore

The enclosed revised report covers the fourth quarter of FY 2000. This report is one of a series to inform the Office of Space and Defense Power Systems, U.S. Department of Energy, and their contractors of accomplishments by the Oak Ridge National Laboratory which is operated by UT-Battelle. If you have any questions or require further clarification on any topic, please contact us at Building 4508, Mail Stop 6079.

JPM:smw

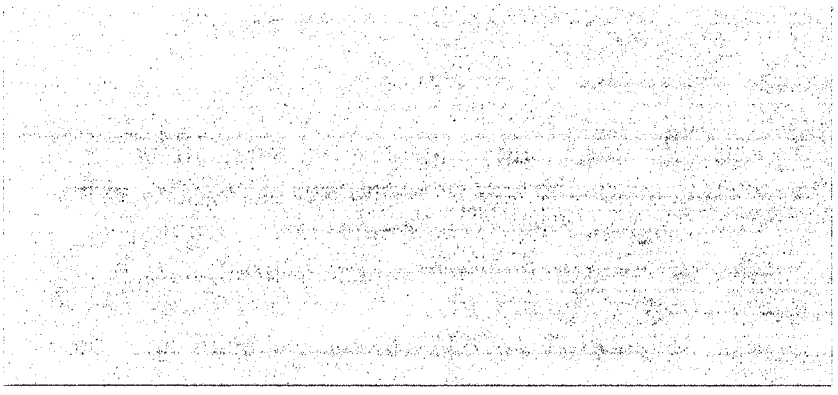

UCN-2383
(3 6-88)

QUARTERLY TECHNICAL PROGRESS REPORT OF RADIOISOTOPE POWER SYSTEM MATERIALS PRODUCTION AND TECHNOLOGY PROGRAM TASKS FOR JULY THROUGH SEPTEMBER 2000

Prepared for Department of Energy
Office of Space and Defense Power Systems
under Budget and Reporting Classification
AF 70 10 20 0, AF 70 60 00 0, and AF 70 30 00 0

by

Radioisotope Power System Program
Metals and Ceramics Division
Oak Ridge National Laboratory

Oak Ridge National Laboratory
Oak Ridge, Tennessee 37831-6080
operated by UT-Battelle, LLC
for the
U.S. Department of Energy
Contract DE-AC05-00OR22725

CONTENTS

1. INTRODUCTION

The Office of Space and Defense Power Systems of the Department of Energy (DOE) provides Radioisotope Power Systems (RPS) for applications where conventional power systems are not feasible. For example, radioisotope thermoelectric generators were supplied by the DOE to the National Aeronautics and Space Administration for deep space missions including the Cassini Mission launched in October of 1997 to study the planet Saturn. The Oak Ridge National Laboratory (ORNL) has been involved in developing materials and technology and producing components for the DOE for more than three decades. For the Cassini Mission, for example, ORNL was involved in the production of carbon-bonded carbon fiber (CBCF) insulator sets, iridium alloy blanks and foil, and clad vent sets (CVS) and weld shields (WS).

This quarterly report has been divided into three sections to reflect program guidance from Office of Space and Defense Power Systems for fiscal year (FY) 2000. The first section deals primarily with maintenance of the capability to produce flight quality (FQ) CBCF insulator sets, iridium alloy blanks and foil, CVS, and WS. In all three cases, production maintenance is assured by the manufacture of limited quantities of FQ components. The second section deals with several technology activities to improve the manufacturing processes, characterize materials, or to develop technologies for two new RPS. The last section is dedicated to studies of the potential for the production of ^{238}Pu at ORNL.

2. PRODUCTION TASKS

2.1 CARBON-BONDED CARBON FIBER

The goal of this effort is to maintain production capability for CBCF insulation sets. These are produced under closely controlled conditions and stringent quality assurance (QA) procedures to ensure compliance with material specifications at each step in the production process, from the handling of raw materials to shipment of finished parts. Dedicated facilities for CBCF production remain in the Carbon and Insulation Materials Technology Laboratory. Periodic exercise of production activities is performed to assure that the processes can be successfully executed and to verify personnel competencies, and adequacy of training, equipment, and procedures.

Our goals this year include (1) complete the fabrication and characterization of CBCF sleeves initiated in FY 1999; (2) produce and certify nine new sets of FQ CBCF sleeves and disks; (3) initiate the qualification of a new, commercially available resin by producing nine sets of sleeves and disks to the current FQ specification; (4) consolidate the storage of CBCF raw materials, archive specimens, and completed sets into a room designated the CBCF Laboratory to allow for greater control and exclusive use of facilities; and (5) initiate preparation of a comprehensive video of all CBCF production and qualification tasks.

2.1.1 Availability of Carbon-Carbon Composites for Radioisotope Power Sources

Current and proposed designs of RPSs are built around the General Purpose Heat Source (GPHS) Module. Each module contains four iridium-alloy-clad isotopic fuel pellets. The combination of the aeroshell, graphite impact shell, and CBCF insulator establishes a suitable operating regime for the fuel clads under both normal and off-normal conditions. The aeroshell and graphite impact shell are made of Textron Fine Weave Pierced Fabric (FWPF) carbon-carbon composite. The performance of this material in GPHS service was established through an extensive program of modeling and testing. Additionally, FWPF has been used extensively for Air Force re-entry applications. Due to a complete collapse in demand, this material has been out of commercial production for nearly a decade. A review was conducted to determine the commercial status of FWPF and to identify a suitable replacement. Textron Systems of Wilmington, MA provided a recent update on FWPF.

FWPF Inventory Status: Textron Systems has four blocks of FWPF in inventory. They measure 5.5 in. square in the X-Y directions by 11 in. long in the Z-direction. Paperwork on these materials is in archive files. Sufficient woven fabric is in inventory to fabricate an additional seven blocks.

FWPF Raw Materials Status: All materials needed for manufacture of FWPF are still available, but additional Hexcel UHM fiber (see below) can only be made on special order with a start-up charge.

FWPF Manufacturing Status: FWPF is manufactured to United States Air Force Specification. It is made using Hercules (now Hexcel) Ultra High Modulus UHM-1K PAN based carbon fiber woven in a plain weave fabric by Textron Products Inc. in Anaheim, CA. The fabric is then cut to size and pierced with steel needles (rods) on Textron systems special looms. The needles are then replaced by pultruded, carbon-phenolic rods to form the dry state undensified 3D architecture. The block is then rigidized using a pitch impregnation and carbonization at Textron's Low-Pressure Impregnation Carbonization (LOPIC) facility. In the past, the rigidized block was then densified by High-Pressure Impregnation Carbonization (HIPIC) at GE / Valley Forge, PA facility, which no longer exists. HIPIC is commercially available at two other qualified facilities. Textron Systems has expressed interest in working with the DOE to reestablish the supply of FWFP.

FMI 223 carbon-carbon composite was identified as a potential alternative for FWPF in the GPHS. FMI 223 is manufactured by Fiber Materials Inc. of Biddeford, ME. This material has also been used extensively by the US Air Force for reentry applications. FMI 223 has been out of commercial production since the early 1990's due to a lack of

demand. Mechanical and thermophysical properties of FMI 223 compare favorably with FWPF. A comparative assessment of FWPF and FMI 223 is the topic of a forthcoming letter report.

FMI 223 Inventory Status: FMI has four blocks of FMI 223 in inventory. They measure 4.8 in. square by 11 in. long in the Z direction. Also in inventory are approximately 5 nosetip-shaped pieces with a minimum diameter of 2.25 in. and an overall length of 10 in.

FMI 223 Raw Material Status: FMI 223 utilizes HMU 1K and 3K fiber that could be made available by special order. FMI has enough fiber in reserve to fabricate six billets.

FMI 223 Manufacturing Status: FMI 223 is made to an Air Force Specification. Currently, there are no anticipated production runs scheduled for this particular material. FMI still has all the processing equipment, preform fabrication tooling and key personnel in place if there was a significant program in place to justify restarting production.

Recommendation: A significant effort has been undertaken to establish FWPF as the material of choice for past RPS systems. I would recommend the purchase of this material in sufficient quantity to justify restart of limited production and to satisfy the anticipated demand for the RPS program over the next ten to twenty years. The Department of Defense could be solicited to determine their near-term demand for FWPF that may allow for cost sharing. Perhaps a significant quantity of this material is held in strategic reserve.

2.2 IRIDIUM-ALLOY BLANK AND FOIL PRODUCTION

The goals for this activity are to produce flight-quality blanks and foil under full configuration control and to supply materials needed for CVS demonstration and maintenance activities. During the second quarter of FY 2000, iridium powder processing and electron beam melting of Ir-0.3% W was performed for the G3 ingot, and 69 blanks from 10 sheets from the G2 ingot were machined.

2.2.1 Blank Fabrication from G2 Ingot

A deviation request to permit the use glow discharge mass spectrographic analysis for thorium in iridium received final approval. The glow discharge mass spectrographic analysis procedure has been used for elements other than thorium for several years and has been used for analysis of thorium in cup d-test samples for the same period. Comparative data on thorium analysis of blanks by this method and the previously used isotope dilution method provided the data needed to justify extension of the glow discharge mass spectrographic analysis method to include thorium. The thorium analyses previously obtained with the Kratos instrument at the Y-12 Plant provided the remaining data needed for blanks from the G2 ingot. A total of 40 prime blanks from the G2 ingot were placed in storage with an approved data package. The blanks are planned to provide 40 blanks during FY 2000 and additional blanks during FY 2001. The six blanks that had been placed on hold following visual inspection were successfully reworked.

Additional glow discharge mass spectrometer (GDMS) analyses were performed on samples of sheets from G2 ingot using the VG9000 spectrometer. These analyses are also all within specification limits. The results indicate that the surface analysis values are effected by the method of cutting the samples. Cutting with the aluminum oxide blade as called for in the current sampling and cleaning procedure does result in elevated values of surface aluminum content. The use of a metal-bonded diamond blade results in lower surface contamination values. The results of these analyses will be used as justification for a future revision of the sampling and cleaning procedure.

2.2.2 Blank Fabrication from G3 Ingot

The G3 electrode was vacuum arc remelted to produce the G3 ingot of 63-mm-diam. The ingot was ground, placed in a molybdenum can, and hot extruded. The extruded bar was cut and cleaned to produce rolling billets for sheet production. Rolling of the billets will be performed during FY 2001. The G3 ingot is planned to yield 90 blanks during FY 2001 and FY 2002.

2.2.3 Arc Melting of Scrap Iridium Ingot

The RS14 scrap alloy ingot melted during the third quarter of this year was sectioned for use in melt stock for a new scrap RS15 electrode. The scrap was button arc melted and drop-cast to produce electrode segments, which were electron beam welded to produce the RS15 electrode. The electrode will be used as needed in the future for practice melting prior to the melting of the FQ material.

2.2.4 Foil Production

Eighteen pieces of foil previously certified to rev. D of foil specification GPHS - M- 186 for fibrous foil were removed from storage and upgraded to rev. E of the specification for recrystallized. The foil was cleaned and recrystallized using an approved special instruction deviation request, examined metallographically, and transferred to the CVS task with a revised data package for use in WS production. Cleaning of witness samples for use in heat treating runs in the CVS task was also completed. The cleaning involves both electrolytic cleaning in KCN solution, rinsing and acid cleaning.

2.3 CLAD VENT SETS AND WELD SHIELD

The goal of this activity is to produce FQ CVS and WS for inventory, test hardware and to maintain the production capability.

2.3.1 Training for FQ Production

The best trained craftsman for frit vent operations retired. Training of a back-up person for the frit vent assembly (FVA) operations was started by producing 12 FVAs. Eight of the twelve (yield of 67%) FVAs had good flow rates. This is lower than the 86% yield by the previous craftsman, but the yield should increase with more experience.

Twelve additional non-FQ blanks (from current process 2.5" diameter ingots RS10 and RS11) as well as 15 FQ blanks were scribed, acid cleaned, welded into blank assemblies, and first-formed. Two new second-form dies were made. One has an inside (forming) diameter of 1.2441" versus the other which has a 1.2448" inside diameter. They both have a 0.300" entrant radius and a 0.38" cylindrical forming surface length. The existing (worn) die from Cassini production has a 1.2458" inside diameter, a 0.325" entrant radius, and a 0.38" cylindrical forming surface length. Initially the new dies had 0.125" entrant radii. Also, initially the 1.2441"diameter die had a 0.8" cylindrical forming surface length.

Forming work with the non-FQ blank assemblies showed that the entrant radius must be larger than 0.125", preferably 0.300 ± 0.025", to avoid complete shearing or gross splitting of the blank assembly at the open end of the formed cup near the top of the iridium. Also, the cylindrical forming surface length does not need to be longer than approximately 0.38". Both the first- and second-form tooling drawings must be modified to show the correct tooling configurations.

2.3.2 Shipping Sleeve Preparation

Over 100 shipping sleeves made from high density polyethylene are being machined. They will be individually scribed with a numerical identity, ultrasonically cleaned in Micro (International Products Corporation, Burlington, NJ) detergent at room temperature and then 100% dimensionally inspected using a coordinate measuring machine. Early work found that properly machined sleeves tend to change dimensions when cleaned ultrasonically at elevated temperature (40° to 60°C), whereas at room temperature they are stable.

2.4 IRIDIUM POWDER AND INVENTORY MANAGEMENT

The purpose of this work is to manage an iridium inventory for all heat source contractors with emphasis on the significant quantities of iridium located at BWXT of Oho, Inc. (BWXT), Los Alamos National Laboratory (LANL), and ORNL, and to maintain a no-change iridium inventory through an annual write-off of inventory and processing losses.

2.4.1 Iridium Accountability Reviews

A review at LANL was conduced on August 8, and 9, 2000. The purpose of this review was to evaluate the accountability, physical inventory, and security of iridium. It was concluded that the accountability for the iridium was in place and operating in a proper manner. No recommendations were necessary.

2.4.2 Iridium Demand and Supply Schedule

The annual update of the iridium demand and supply schedule is summarized in Table 1. This schedule, which is prepared for contingent planning purposes, presents a strategy to assess the availability of iridium for all improving and producing activities by projecting future demands. Using this schedule enables us to project an adequate supply to meet our current and future needs. An adequate inventory needs to be maintained due to potential follow-on missions after Cassini, for which the production of blanks and foil was completed in FY 1996. The hypothetical missions assume a need for the yearly quantities of blanks and foil in the schedule for FY 2000 through FY 2003.

The first part of the schedule shows the production demand factors for FQ blanks and foil. The schedule of produced blanks and foil represents the quantity and timing for delivery or storage at ORNL. The ingots from new material represent the quantity produced from new iridium powder to make either blanks or foil. These ingots must be produced on a timely basis to meet the lead-time requirement to produce and deliver or store the blanks and foil.

The production of the FQ blanks and foil produces recyclable iridium material that can be placed back into the production process at ORNL. A greater economic benefit is realized by using recycled material, since the need to purchase powder from an outside vendor is reduced.

Refineable iridium scrap is also generated from the production of FQ blanks, non-FQ blanks, and foil. This scrap is sent to a commercial refinery when a sufficient accumulation occurs at ORNL and funding is available for the refining.

Process losses of iridium occur during the working of the material at ORNL, BWXT, and LANL. Losses also occur during the refining process. These inventory losses are written-off annually.

No refining contracts and no new purchases of iridium powder are planned at this time, as shown in the supply strategy portion of the table. The available recycle material and scrap has been considered to have been already recycled before calculating how much powder needs to be purchased.

To summarize the information contained within the table, there is an adequate supply of iridium powder to produce the hardware for the hypothetical follow-on missions after Cassini.

Table 1. Demand and Supply Schedule Shows Factors and Provides Strategy to Ensure an Adequate Supply of Iridium Powder for Potential Follow-On Missions After Cassini

Factors and strategy	U. S. Government fiscal years			
	FY 2000	FY 2001	FY 2002	FY 2003
Production-demand factors				
Produced blanks	40	40	40	80
Ingots from new material	1	0	1	0
Ingots from recyclable material	0	1	0	1
Produced foil (m^2)	0	0.1	0	0
Refining and process losses (kg)				
Refining loss	0	0	0	0
Processing losses	1	2	2	2
Supply strategy (kg)[1]				
Beginning balance of powder	87	70	70	57
Receipt of refined powder	0	0	0	0
Receipt of purchased powder	0	0	0	0

[1]FY 2004 beginning balance of powder is estimated to be 57 kg.

2.5 SHIELD CUP MODIFICATION

The goal of this activity is to widen the vent notches and install the integral WS in 59 FQ and 9 EU shield cups returned from LANL. Also, WSs must be installed in the 14 Qualification Production shield cups and then the shield cup assemblies (SCA) must be re-matched with the VCA's.

2.5.1 Establishing Capability for Installing IWS

The CVS Cleaning Area in Building 2525 at ORNL was re-opened after it had been shutdown temporarily for approximately 3 weeks because of housekeeping and safety concerns. The 3 CVS manufacturing procedures (GPHS-Y-005, -006, and -007) that require the use of acids were revised (DR-CVS-024) to state more clearly the specific types of chemical protective clothing that are to be used. These procedure modifications along with additional job hazard evaluations were done as part of the resumption of operations in the CVS Cleaning Area.

Two additional copies of the WS tab-to-shield cup weld fixture were successfully fabricated. New springs (7/16" long) were put in all 3 fixtures to ensure full travel for the tab hold-down fingers so that the WS tabs will always be held against the inside of the cup wall during welding.

2.5.2 Processing of LANL Returns and Qualification Production Assemblies

Four EU and five FQ shield cups returned from LANL were completed as SCAs per the special instruction deviation request, SIDR-CVS-003. C. E. Grosso and M. O. Smith of Westinghouse Government Services Group performed a follow-up assessment of the ORNL WS and shield cup assembly production preparedness on August 17, 2000. They examined the completed 4 EU and 5 FQ SCAs and reviewed the manufacturing records, procedures, deviation requests, and equipment. The Westinghouse personnel recommended to the DOE Office of Space and Defense Power Systems that ORNL be given permission for full WS and shield cup assembly production.

Shortly after the review and recommendation by Westinghouse personnel, the DOE Office of Space and Defense Power Systems granted permission for ORNL to begin full WS and SCA production. A total of 123 FQ integral WSs (3620-01) were initiated. Thirty one of these were scrapped for a yield of 75%. Twenty two were scrapped for weld burnback which must not exceed 0.64 mm at either end. As production proceeded and the welder gained experience less burnback problems were encountered. Eight WSs were scrapped for cracks in tab radii that appeared after forming. These cracks were most likely related to the soundness of the stamped edges which is tied to foil/tooling conditions.

WSs have been welded into all 14 Qualification Production shield cups along with the 9 EU and 59 FQ shield cups returned from LANL. Rewelding must occur on 3 FQ shield cups because of minor cracking in some tab welds that extends slightly into the cup base metal. All SCAs must be processed through air burn-off, vacuum outgassing, weld inspection, and dimensional inspection prior to certification review. Once the certification review is complete, the shield cups from LANL will be ready for shipment. The Qualification Production SCAs must be re-matched with their VCAs before shipment probably in late December.

3. BASE TECHNOLOGY PROGRAM AND TECHNICAL SUPPORT ACTIVITIES

3.1 TECHNICAL SUPPORT FOR ADVANCED RADIOISOTOPE POWER SYSTEM (ARPS) AMTEC CELL DEVELOPMENT

3.1.1 Introduction

The Alkali Metal Thermolelectric Converter (AMTEC) cell is one of the primary thermal to electric conversion technologies being considered for future NASA outer planetary space missions. These cells use refractory metal alloys as materials of construction and sodium (Na) as a working fluid. ORNL is providing technical support to the AMTEC development program by providing materials fabrication, mechanical property data support, and component joining fabrication with the electron beam (EB) welding process. Nb-1Zr has been the primary material for the cell components developed for the ARPS Program. Oxidation concerns with this alloy have lead to the study of Mo-41Re as an alternate material. Mo-Re alloy sheet is being produced for evaluation in AMTEC development cells. Oxidation studies are being conducted on materials for the AMTEC application.

3.1.2 Oxidation Studies

Recent oxidation testing has focused on long-term tests in low P_{O_2} vacuum or argon, and Table 1 summarizes the results that have been obtained on Mo-41%Re since the last quarterly report. One observation is that the long-term weight gain rate at 900°C is lower than at 800°C. Previously, this same type of anomaly was found in 500 h tests, although the difference after 500 h was closer to a factor of two than the factor of five after 1,000 h. Furthermore, in argon at 800°C and a much higher partial pressure of oxygen, the weight change rate after 1000 h was only a factor of three higher than in vacuum (P_{O_2} = 1 x 10^{-6} torr), even though the partial pressure in argon was more than a factor of 1,000 higher. Previous results at high temperatures (800-900°C) in vacuum have shown that high pressures cause net weight losses instead of gains.[1]

Table 1. Weight change rate of Mo-41%Re

Time (h)	Temperature (°C)	P_{O_2} (torr)	Weight change rate (mg/cm^2-h)
500	600	1 x 10^{-5}	4 x 10^{-5}
1,000	800	1 x 10^{-6}	2.3 x 10^{-4}
1,000	900	1 x 10^{-6}	4 x 10^{-5}
1,000	800	3 x 10^{-3} (Ar)	6 x 10^{-4}

Even though the above observations are not well understood, the low rates of weight gains that have been measured after long times in these pressure ranges continue to support the proposition that, with proper precautions, Mo-41Re should have satisfactory oxidation resistance for ARPS applications.

3.1.3 AMTEC Cell Fabrication Development

Fabrication support to AMPS continued during this reporting period for the development of the AMTEC cell. Welding fabrication of AMTEC cell components for the EPX-01-E5SA2 was completed. The cell was tested and no detectable leaks were found in the assembly at ORNL. A computed tomography scan was performed to characterize the internal components.

ORNL visited AMPS to discuss issues and plan program objectives for the development of a chimney design AMTEC cell with Mo-41%Re as the primary material. This was a successful meeting that identified some of the material and technology needs for the program planned for the next two years. Some of the various product forms of Mo-41Re required for processing cell components were determined and these include round bar, sheet, plate, and wire. Brazing technology development of Mo-41%Re to ceramic insulators is one of the areas of high priority for AMTEC cells. Sheet

material of Mo-41%Re was supplied to AMPS for preliminary brazing trial assessment using vanadium at their vendor who is currently brazing feedthroughs on Nb-1Zr cells.

A test weldment in nominally 0.5 mm thick sheet was made with the electron beam process as a preliminary assessment of joining Mo-41%Re to pure Nb. This dissimilar metal combination has been proposed as a joint between a BASE tube flange and the BASE support plate. The weld exhibited some transverse cracks as-welded and very low ductility on bending at room temperature. This initial test raises concern about using this material combination in the cell design.

A summary report, "Production and Properties of Mo-41%Re for AMTEC Cell Construction" was written to transfer the available information on this material to AMPS and other program participants. This report summarizes the work conducted for the production of the Mo-Re alloy, the fabrication characteristics of the alloy, compatibility of the alloy with sodium and oxygen, and the mechanical and physical properties which have been measured or obtained from the literature.

3.1.4 Molybdenum-41% Rhenium Alloy Sheet and Foil Production

The goals for this activity are to produce Mo-41% Re sheet for AMTEC demonstration cells. During the fourth quarter of FY 2000 extrusion of the MR3 ingot was completed. Vacuum arc remelting of the MR4 ingot and preparation of the MR5 electrode were also completed. Powder processing and electron beam melting of the MR6 electrode was initiated.

MR3 ingot was placed in a thin-wall (1.6 mm) molybdenum can, which was sealed by electron-beam welding. The can was induction heated in argon to a temperature of 1850°C as measured by a two color optical pyrometer. The billet temperature inside the can is estimated at 1750°C on the basis of a previous calibration using a Type C thermocouple in contact with the Mo-Re billet. The heating time from room temperature to 1850° C was approximately 90 minutes and was followed by a hold at temperature of 5 minutes. The billet was then removed from the furnace and extruded through a zirconia-coated die with a rectangular die opening of 19 by 51 mm. The extrusion exhibited a smooth surface free of the surface tears along grain boundaries observed previously with extrusion of uncanned Mo-Re ingots. This is attributed to the exclusion of oxygen from the deforming material surface. Chemical analysis of samples from opposite ends of the extruded bar indicates interstitial contents of 72 and 87 ppm carbon and 3 and 2 ppm oxygen respectively. These values are well within the desired range.

A total of 12 kg of blended Mo-41%Re powder for ingot MR4 was electron beam melted. Carbon was added using a master alloy. The master alloy was prepared with an addition of 7700 ppm carbon and was analyzed by Leco analysis at CSM Inc. at 7050 ppm. Carbon-containing alloy bars with analyzed carbon contents of about 450 ppm were prepared and used together with low carbon (<20 ppm) alloy bars for assembly of a VAR electrode. The electrode was assembled by welding in the electron beam furnace with the carbon-containing bars placed end to end along the centerline of the electrode. The calculated average carbon content of the electrode was 90 ppm. The electrode was vacuum arc remelted to produce an ingot of 84-mm-dia. and a molybdenum extrusion can prepared. Extrusion of the MR4 ingot was delayed until more definite information on the required product forms could be obtained.

A total of 13.5 kg of Mo-41%Re powder for billet MR5 was blended, compacted, sintered and electron beam melted. An electrode for vacuum arc remelting was fabricated using a calculated carbon addition of about 85 ppm. The carbon is added as a master alloy produced from spectrographic carbon rod with a master alloy of about 5000 ppm, in the same manner as for the MR3 and MR4 electrodes. Powder blending, compacting, sintering and electron beam melting of a total of 13.5 kg of Mo-41%Re powder for billet MR6 was initiated. A total of 14 kg of rhenium powder was purchased to permit the fabrication of 2 additional ingots.

3.2 ALLOY DEVELOPMENT AND CHARACTERIZATION

3.2.1 Effect of Aging on the Intermediate-Temperature Tensile Ductility of Haynes Alloy 25

Haynes-25 alloy is to be used as a pressure vessel in the Advanced Long Term Battery Heat Source [1]. Much of the currently-available mechanical properties data on Haynes 25 was generated several decades ago [2] and it is well known that there is a trough in the tensile elongation versus test temperature curve at intermediate temperatures [2,3]. The mechanism responsible for this decreased ductility is not understood but may be related to precipitate dissolution, formation, or growth as a result of aging at these temperatures. Other possibilities to consider include environmental embrittlement (by oxygen) and increased propensity for grain-boundary fracture at intermediate temperatures. A new heat of Haynes alloy 25 has been produced for use in the heat source and it was judged necessary to re-evaluate its properties using specimens from that heat. A previous study characterized the intermediate-temperature ductility loss in this alloy with respect to test temperature, strain rate, and environment [4]. The results showed that the ductility trough in the new heat of Haynes 25 occurs at temperatures of approximately 600 to 825 °C. The results of tests at strain rates between 1 x 10^{-2} and 3.3 x 10^{-5} s^{-1} suggested a possible connection to environment since ductility increased with increasing strain rate. The purpose of this study is to investigate the effect of aging at 550 and 850 °C in order to determine if precipitate formation and growth play a role in the intermediate temperature ductility loss.

Haynes 25 sheet stock (~3.5 mm thick) was received from BWXT in the solution-annealed and recrystallized condition, having an ASTM grain size of 4-5 (~60-90 μm). Tensile specimens with a gage cross section of 0.6 x 2.5 and gage lengths of 12.7 or 11.4 mm were machined and the surfaces were ground through a 600-grit SiC finish. The samples were then encapsulated in an argon-filled pyrex tube and heat treated at 550 or 850 °C for times up to 2015 h. The aging times chosen are marked with an "x" in the time-temperature-transformation diagram (TTT) for Haynes 25 shown in Fig. 1 [5] and were selected to coincide with the different types of precipitates that form in this system. Tensile tests were conducted in vacuum (better than 10^{-5} torr) at 750 °C at a strain rate of 10^{-3} s^{-1}. One additional test was conducted at a strain rate of 10^{-5} s^{-1}. Only one test at each condition was performed. Tensile ductilities were determined by measuring the total specimen length before and after testing and assuming that all the elongation occurred in the gage section. Scanning electron microscopy was used to determine the fracture modes.

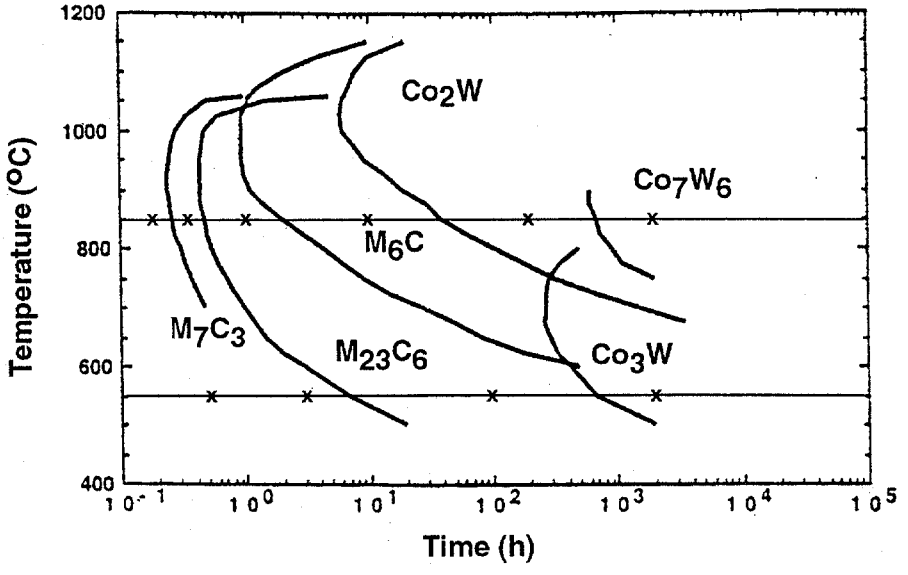

Fig. 1. Time-temperature-transformation diagram for Haynes 25 [5].

Our previous study [4] showed that the intermediate temperature ductility loss in the BWXT heat of Haynes 25 occurs at temperatures of 600-825°C, with the minimum occurring at approximately 750-775°C. Therefore, for the current tests, 750°C was chosen as the temperature for further study of this phenomenon. Table 1 shows the results of tensile tests in vacuum at a strain rate of 3.3×10^{-3} s^{-1} for Haynes 25 samples aged for various times at 550 and 850°C. For samples aged at 550°C, aging times of up to 2015 h did not appear to affect the tensile strength or ductility. The yield strength varied from 248 to 270 MPa, the ultimate strength from 562 to 618 MPa and the elongation to fracture from 42.5 to 45.6%. All these values are comparable to values measured previously at 750°C for as-received alloy [4] and to data compiled for a large number of commercially-produced Haynes 25 heats [2]. For specimens aged through 210 h at 850°C, yield and ultimate strengths and elongations were also comparable to those specimens aged at 550°C, although the scatter in the data for those aged at 850°C was much larger. Values ranged from 236-273 MPa, 523-668 MPa, and 42-60.2% for the yield strength, ultimate strength, and elongation, respectively. Aging for 2015 h at 850°C resulted in a decrease in the elongation to failure (Fig. 2) and a slight increase in the yield strength. All of the samples aged at 550°C and the samples aged through 210 h at 850°C work hardened during tensile testing until very near fracture (through elongations of greater than 40%). The sample aged for 2015 h at 850°C, on the other hand, work hardened through an elongation of only about 20%, then failed at an elongation of 28.7%. In terms of its effect on the intermediate temperature tensile ductility minimum, the data in Fig. 2 suggest that aging at 550°C for the times used in this study or at 850°C for times up to 200 h had no effect. Aging at 850°C for times of less than about 100 h may actually enhance the ductility slightly. However, longer aging times at 850°C, which result in the formation of Co-W-based precipitates, tend to decrease the ductility.

Table 1. Elongation and Strength of Aged Haynes 25 Tensile Tested at 750°C

Aging Temp.(°C)	Aging Time (h)	Tensile Strain Rate (s^{-1})	Yield Strength (MPa)	UTS (MPa)	Elongation (%)
550	0.5	3.3×10^{-3}	269	605	42.5
	3		248	603	42.6
	100		263	562	45.6
	2015		270	618	45.2
850	0.2	3.3×10^{-3}	268	668	52.9
	0.35		268	630	46.1
	1		236	523	52.9
	10		244	597	60.2
	210		273	634	42.0
	2015		317	607	28.7
850	2015	3.3×10^{-5}	316	394	36.2

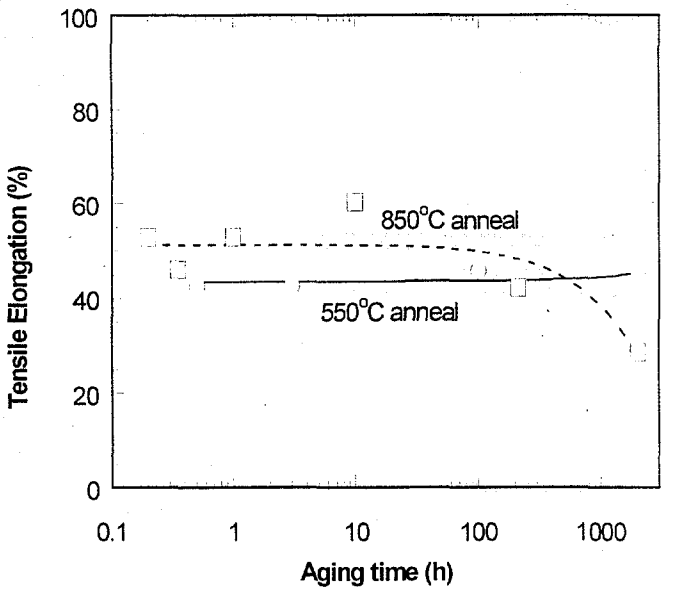

Fig. 2. Effect of heat treatment on the tensile elongation of aged Haynes alloy 25 tested in vacuum at 750°C and a strain rate of 3×10^{-3} s^{-1}.

Figure 3 shows fracture surfaces of samples aged at 850°C for 10 and 2015 h. The sample aged for 10 h showed macroscopic evidence of necking (Fig. 3a) and failed in a ductile dimple mode (Fig. 3b). Small precipitates were visible in the bottom of many of the dimples. The sample aged for 2015 h at 850°C exhibited basically the same type of failure (Fig. 3c), but the precipitates in the bottom of dimples were larger and the dimples themselves appeared somewhat truncated (Fig. 3d). Compared to the fracture mode of the as-received Haynes 25, which was predominantly grain boundary failure [4], the fracture surfaces of the aged samples contained only a small percentage of fracture along grain boundaries.

The sample aged for 2015 h at 550°C fractured in a mixed mode of ductile dimple and grain boundary failure (see Fig. 4). Precipitates were not generally observed in the dimples and only a few were present on grain boundary facets.

One specimen aged for 2015 h at 850°C was also tensile tested at the slower strain rate of 3.3×10^{-5} s^{-1} and the results are included in Table 1. This specimen had a yield strength and ductility comparable to the 2015-h aged specimen tested at the higher strain rate, but it exhibited very little work hardening and had an ultimate tensile strength of only 394 MPa. Figure 5 shows that it failed through a creep-like mechanism with many creep-induced cavities visible on the fracture surface. Metallography of the gage of this specimen (Fig. 6) showed that the creep cavities formed on the grain boundaries next to the W-enriched precipitates. The elongation to failure for the 2015h/850°C-aged specimens tested at both the slow and fast strain rates are compared in Fig. 7 to the ductility versus strain rate data produced earlier for as-received Haynes 25 [4]. The two data points for aged Haynes 25 suggest that long-time aging at 850°C causes embrittlement at the high strain rate but not at the slow strain rate. More tests are planned to determine the effect of strain rate on ductility of aged specimens.

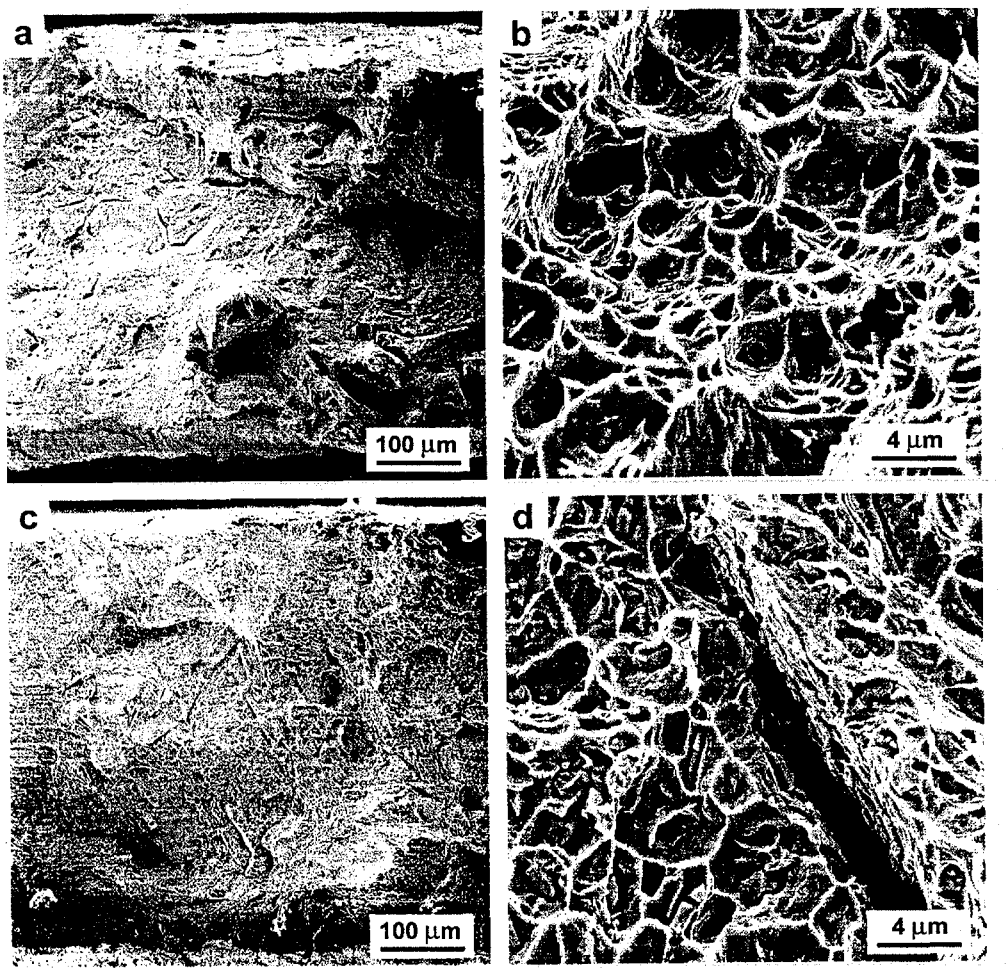

Fig. 3. Scanning electron fractographs showing tensile fracture modes of Haynes Alloy 25 tested in vacuum at 750°C after aging at 850°C for (a,b) 10 and (c,d) 2015 h.

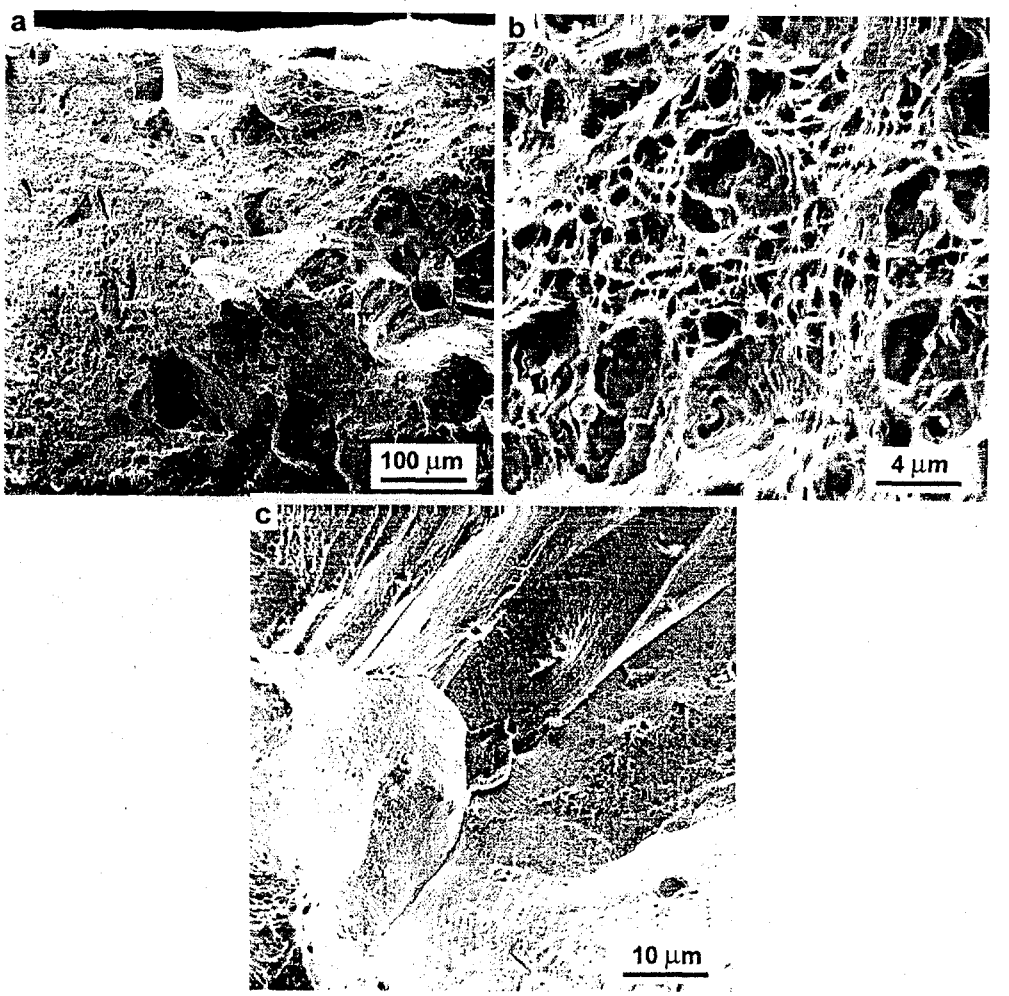

Fig. 4. Low magnification fractograph (a) and high magnification fractographs of two different regions (b,c) of the fracture surface of Haynes 25 aged for 2015 h at 550°C and tensile tested at 750°C at a strain rate of 3.3×10^{-3} s^{-1}.

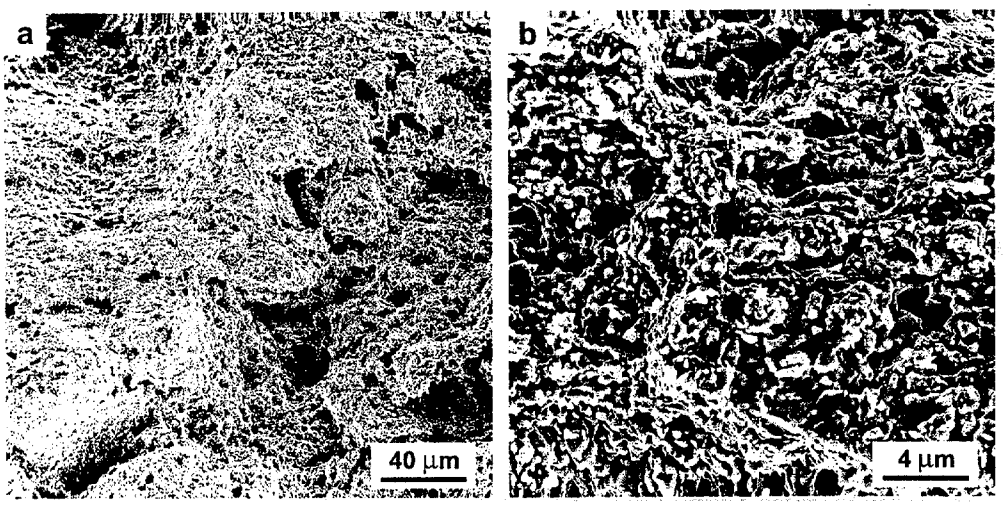

Fig. 5. Low (a) and high magnification (b) fractographs of Haynes 25 aged 2015 h at 850°C and tensile tested at 750°C at a strain rate of 3.3 x 10^{-5} s^{-1}.

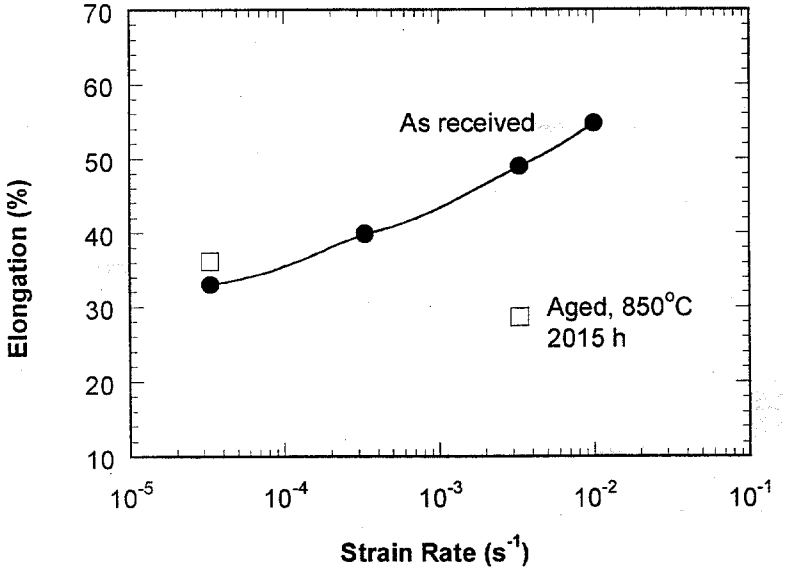

Fig. 7. Effect of heat treatment and strain rate on tensile elongation of Haynes Alloy 25 tested in vacuum at 750°C.

(a) (b)

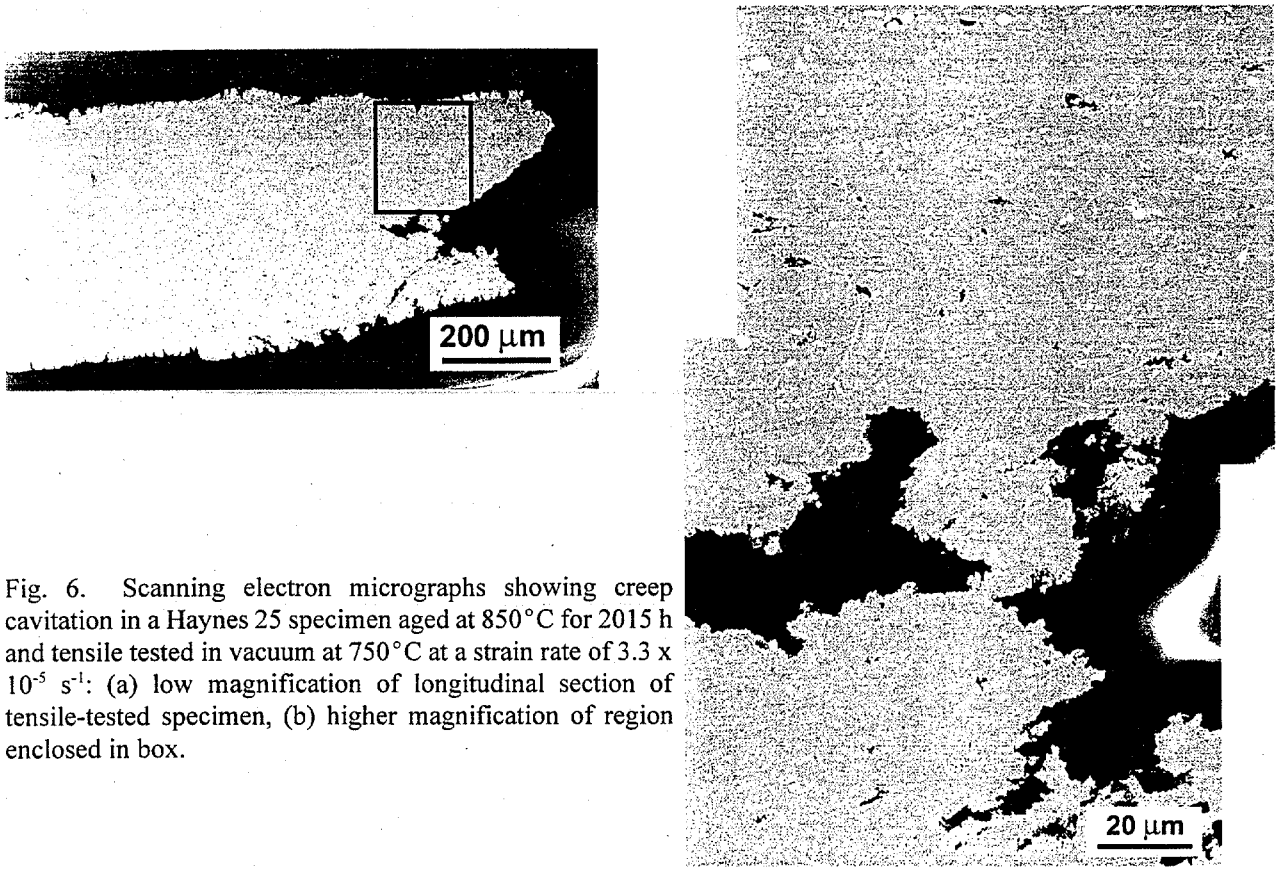

Fig. 6. Scanning electron micrographs showing creep cavitation in a Haynes 25 specimen aged at 850°C for 2015 h and tensile tested in vacuum at 750°C at a strain rate of 3.3 x 10^{-5} s^{-1}: (a) low magnification of longitudinal section of tensile-tested specimen, (b) higher magnification of region enclosed in box.

In summary, the effect of aging at 550 and 850°C on the intermediate temperature tensile ductility minimum in Haynes 25 was studied. Samples were aged for up to 2015 h and their tensile properties at 750°C (in the ductility trough) were compared to those of as-received Haynes 25. Aging at 550°C for times of up to 2015 h did not appear to affect the tensile strength or ductility. The yield strength ranged from 248 to 270 MPa, the ultimate strength from 562 to 618 MPa and the elongation to fracture from 42.5 to 45.6%. Aging through 210 h at 850°C resulted in strengths and elongations comparable to those of specimens aged at 550°C. In fact, the ductility may have been slightly enhanced by aging for short times at 850°C, as elongations to failure of 42-60% were observed. However, specimens aged for 2015 h at 850°C exhibited reduced ductilities and may indicate that formation and growth of Co-W-based precipitates affect ductility in long-term-aged specimens. This is similar to the embrittling effect of aging seen in impact-tested specimens [6].

The study of the effect of aging on medium- and high-strain-rate tensile properties will continue. Longer-term aging treatments at 850°C have been started. Studies are also planned to investigate the effects of additional aging temperatures and tensile test conditions.

References

1. T. J. Dobry and S. T. Christenbury, "Advanced Long Term Battery Isotopic Heat Source Test Plan" (TES-21501-114) July 11, 2000

2. R. W. Swindeman, "Review of the Mechanical Behavior of Haynes Alloy No. 25," Oak Ridge National Laboratory, July 15, 1998.

3. T. Lyman et al., editors, Metals Handbook, Vol. 1, 8th Edition, American Society for Metals, Metals Park, OH, 1961, p. 522.

4. C. G. McKamey, J. L. Wright, E. H. Lee, and E. P. George, "Characterization of the Tensile Ductility Loss at Temperatures of 600-900°C in Haynes Alloy 25," attachment to letter, J. P. Moore to W. J. Barnett, Sept. 30, 1999.

5. N. Yukawa and K. Sato, pp. 680-66 in Proceedings of the International Conference on the Strength of Metals and Alloys, The Japan Institute of Metals, Omachi, Japan, 1968.

6. C. G. McKamey, E. H. Lee, J. L. Wright, and E. P. George, "Effect of Aging on Tensile Impact Ductility of Haynes Alloy 25," attachment to letter, J. P. Moore to W. J. Barnett, July 31, 2000.

3.3 TECHNICAL SUPPORT FOR ADVANCED LONG TERM BATTERY

3.3.1 Background

The fuel in the advanced long term battery will be contained within nested capsules fabricated from Haynes Alloy No. 25. This material is a solid solution cobalt base alloy with excellent fabricability, corrosion resistance, and mechanical strength. Although the alloy was used several decades ago for fuel encapsulation, re-evaluation and qualification of a newly-produced heat was judged to be an essential part of the safety test plan for the battery (ref. 1). A large heat of Haynes 25 was procured for all testing and evaluation. ORNL was given the responsibility for producing the mechanical properties needed for the evaluating the lifetime of welded capsules under envisioned conditions of temperature, pressure, and age. The test plan identified uniaxially-stressed tensile, creep-rupture, and low-stress creep tests on base metal and weldments. As-received and aged materials were included in the testing plan. About 60 tests on base metal and 60 tests on weldments were specified (1). Pressurized capsule tests were identified in the plan. To meet the testing performance standards required for a safety analysis, testing equipment assigned to the program had to be updated and the standard operating guidelines had to be revised and critically reviewed.

3.3.2 Material and Specimens

The material and specimens for tensile and creep testing were described previously (2). The ladle chemistry reported by the vendor was as follows: 11% C; 20.23% Cr; 2.34% Fe; 1.51% Mn; 10.32% Ni; 0.008% P; 0.002% S; 0.16% Si; 14.77% W; balance Co. The grain size was ASTM No. 4. The material was in the annealed condition.

Tensile and creep sheet specimens were identical and had a reduced section 2.14 inches (54.3 mm) long, 0.4-inch (10-mm) wide, and 0.14-in. (3.56-mm) thick.

Ten welded plates of Haynes 25 for the fabrication of weldment samples were received from BWXT. The dimensions of the plates were 7 inches by 12 inches (178 mm by 305 mm) by 0.14 inch (3.56 mm) thick. The weld was located in the center of the 7-in. (178 -mm) dimension and parallel to the 12-in. (305-mm) edges. Distortion, normally associated with welding plates of this thickness, produced a kink in the 7-in. (178-mm) direction of a few degrees across the weld from one half plate to the other. Seven weldment specimens were cut from each plate and these were orientated such

that the weld would be at the center of the reduced section and perpendicular to the loading axis. The sketch in Fig. 1 shows the orientation of the specimen blanks. We were concerned that the kink retained in machined specimens might affect the mechanical performance of the weldment specimens. An option was to flatten the specimens prior to aging and testing, so exploratory testing was undertaken to examine the consequences of flattening. Some machined samples were flattened in a three-point bend rig. An as-machined weldment specimen, a flattened weldment specimen, and a base metal specimen were embrittled by aging for 92 hours at 850°C, then tensile-tested at room temperature. All aged specimens showed about the same embrittlement, as indicated in Table 1, and failures occurred in the base metal away from the weld. The ultimate strength of the weldment specimens was lower than the base metal for both the mill and aged conditions. It is not known whether the lower tensile strength was a result of restraint imposed by the weld or bending stresses related to the kink. However, the flattened weldment specimen was slightly stronger and more ductile than the unflattened specimen, so the flattened condition was judged to be more typical of the capsule weld and not detrimental to the tensile properties. Test specimens were ordered.

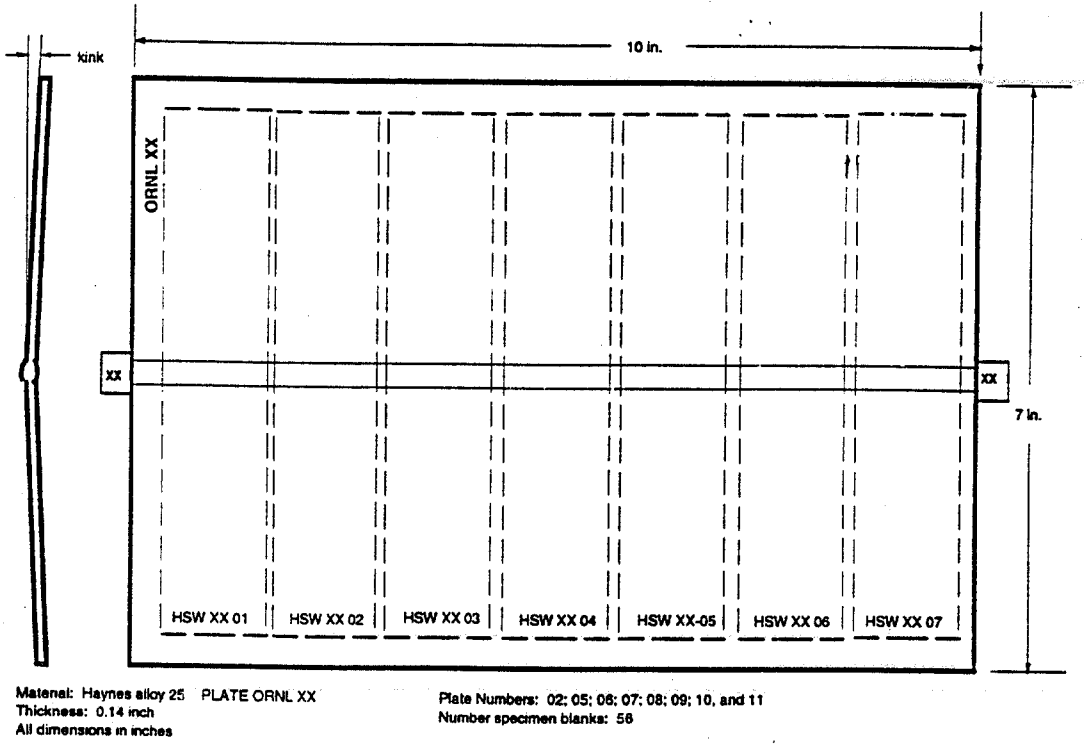

Fig. 1. Cutting plan for weldment specimen blanks.

Table 1. Results of Tensile Tests to Examine the Influence of Flattening of Weldment Specimens

Specimen	Condition	Ultimate Strength (ksi)	Elongation (%)	Failure Location
HS 02-01	Base	145	56.6	Base
HS 03-30	Base + age	153	26.0	Base
HS25W03	Weld + age	128.9	21.1	Base
HS25W01	Weld + flatten + age	134.0	25.2	Base

3.3.3 Effect of Aging on Tensile Properties

The results of the tensile testing of the mill-annealed material were reported previously. A summary of the tensile data for material aged for 6000 hours is provided in Table 2, and plots of properties versus temperature are shown in Figure 2 and 3. Data for the mill and aged conditions are compared in these figures. In Figure 2, it may be seen that the yield strength is significantly increased to 800°C by aging. To a lesser extent, the ultimate strength was also increased by aging. The strengths for the two conditions coverged above 800°C and were virtually the same at 1000 and 1100°C. Ductility data, plotted in Figure 3, indicated that aging significantly reduced ductility relative to the mill condition at all temperatures. Both the elongation and reduction of area increased with increasing temperature but never reached the values typical of the mill condition. Nevertheless, the ductility for the aged material was judged to be within the range of expectations based on literature data. Specimens aged 12,000 hours at 675°C were removed from the aging furnace and prepared for tensile testing.

Table 2. Tensile Properties for Haynes Alloy 25 Aged 6000h at 675°C

Test Number	Specimen Number	Temp. (°C)	Proportional Limit (ksi)	Yield Strength (ksi)	Ultimate Strength (ksi)	Uniform Strain (%)	Elongation Strain (%)	Reduction of Area (%)
29760	HS 02-10	23	53.0	114.5	152.7	7.3	7.3	4.4
	HS 02-16	23	79.6	114.9	151.5	8.4	8.4	5.8
29761	HS 02-14	300	55.0	88.5	138.5	13.7	13.7	13.8
29762	HS 02-09	500	61.0	81.0	137.1	17.3	17.3	16.1
29763	HS 02-13	650	49.0	74.8	131.5	21.3	21.3	14.7
29764	HS 02-11	800	39.0	64.6	81.9	3.6	17.3	16.6
29765	HS 02-15	1000		25.8	25.9		45.2	39.0
29766	HS 02-12	1100	9.0	14.7	14.7		47.9	32.9

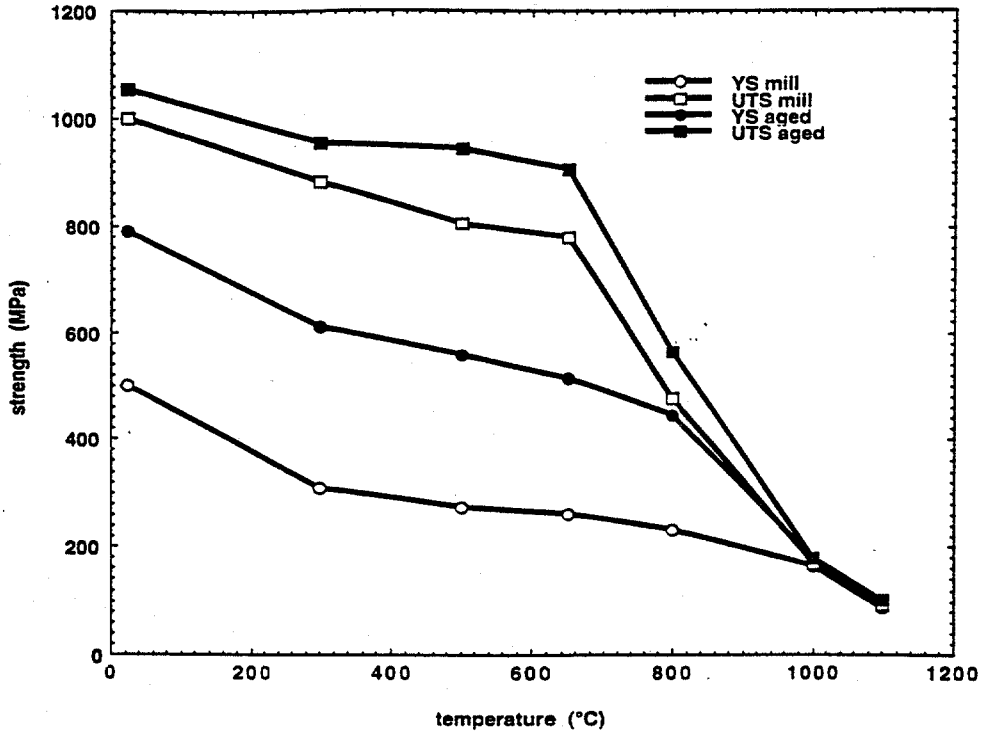

Fig. 2. Comparison of tensile strengths for mill and aged HS 25.

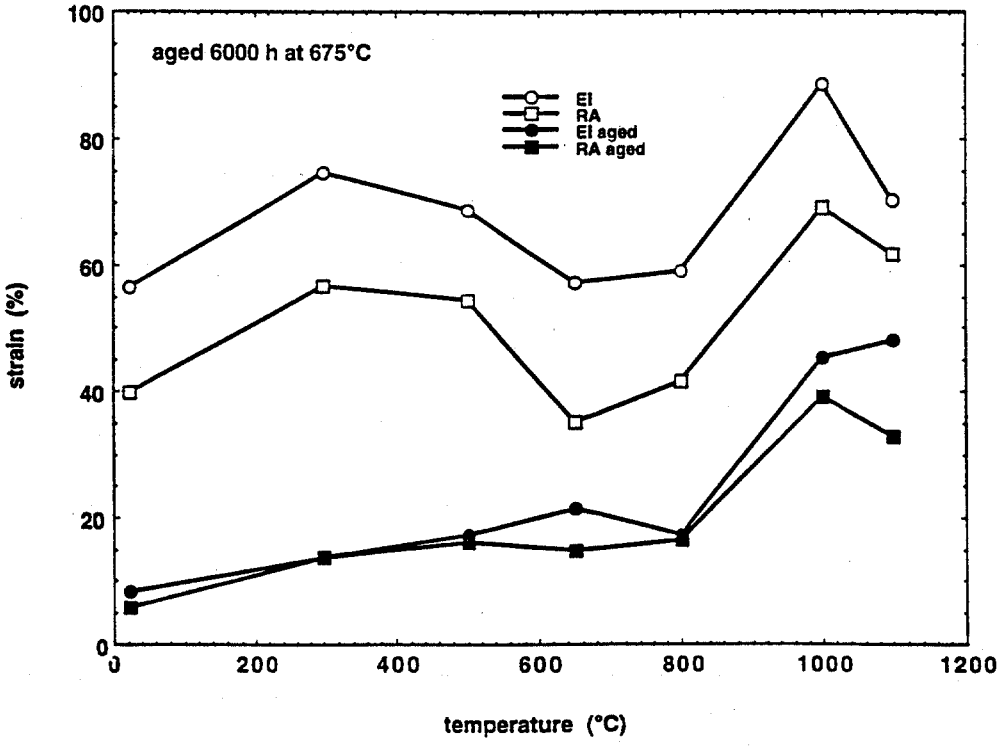

Fig. 3. Comparison of tensile ductility for mill and aged HS 25.

3.3.4 Creep-Rupture Testing

Several of the creep-rupture tests (CR-series) identified in the test plan were started, and results are summarized in Table 3. Temperatures ranged from 650 to 850°C and the longest testing time exceeded 4000 hours. The minimum creep rate usually occurred beyond 1000 hours. A comparison was made between the observed creep rate and the estimated creep rate provided in the test plan (1). The results are shown in Figure 4. The observed creep rates were about 20% higher than the estimated rates. An exception was specimen CR-BM-02 tested at 700°C and 24 ksi (165 MPa) which crept four times faster than expected. This test accumulated less than 1000 hours, so the creep rate may diminish significantly with time and approach the estimated value in the test plan (1).

Table 3. Summary of Creep Rupture Tests on HS 25

Test Number	Temperature (°C)	Stress (ksi)	Time in Test (h)	Creep Strain (%)	Creep Rate (%/h)	Status
BM-CR-01	650	30	3200	0.8	0.00017	primary ?
BM-CR-02	700	24	800	1.2	0.0012	secondary ?
BM-CR-03	750	18.5	4000	3.4	0.00053	secondary ?
BM-CR-04	800	14.4	4200	4.2	0.0008	secondary ?
BM-CR-05	800	15	3700		0.0011	ruptured
BM-CR-06	850	9	4100	1	0.0001	primary
MG-21	650	27	3800	0.8	<0.00015	primary
MG-22	675	15	100	0.05		primary

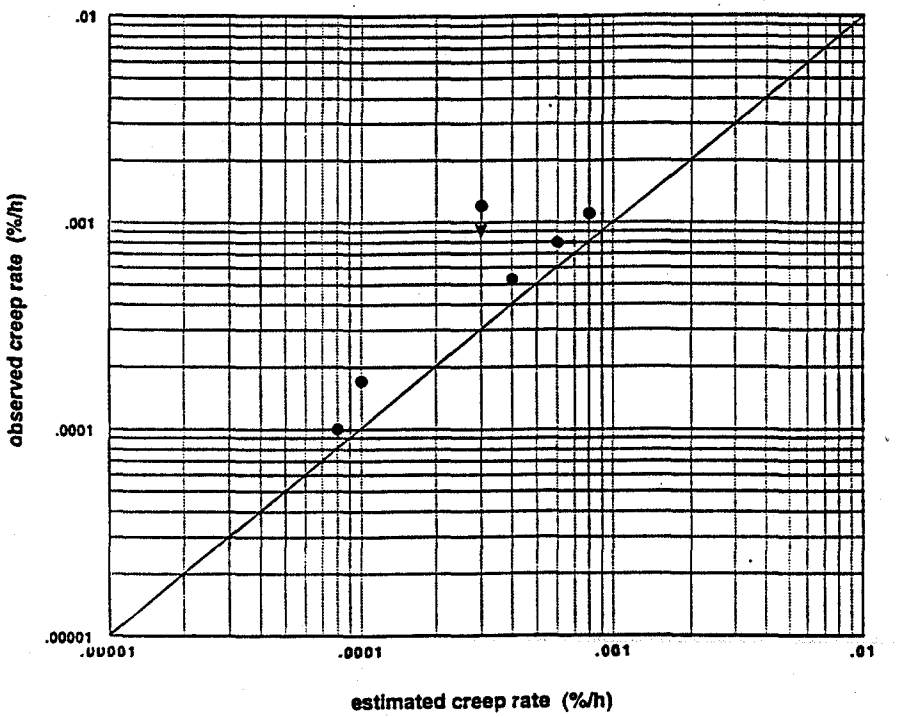

Fig. 4.. Observed versus estimated creep rates for HS 25.

3.3.5 Creep-Rate Testing

Two creep-rate tests (MS series) were started, and results are summarized in Table 3. Comparison of the creep curve for MG-21 with the curves published by Widmer, et at. (4) indicated reasonably good agreement.

3.3.6 Pressurized Capsule Testing

The pressurized tube testing facility was modified to permit the testing of capsules to pressures of 7000 psi (48 MPa) and temperatures to 950°C. A sketch of the test capsule within the canister if shown in Fig. 5. The canister is a 3.5-in. (90-mm) diameter 304L stainless steel can. The lid contains penetrations for the test capsule pressure tube, three thrermocouple wells, three sheathed thermocouples, and cover gas inlet and outlet tubes. A guard heater may be placed around the canister at any axial location to regulate the temperature profile. The canister is suspended from clamps placed on the cover gas tubes. A sketch of one of the test stations is provided in Figure 6. Here, the test capsule assembly is shown within a tubular furnace and the pressurization lines and inert cover gas lines are shown above the furnace. High-pressure gas (argon plus 5% helium) is brought to the test capsule through valve J. The pressure within the test capsule is monitored by a pressure sensor gage. The cover gas (argon) flows through the canister at a controlled rate. The outlet for the cover gas line can be checked for the presence of helium that can only be present if a crack penetrates the wall of the capsule. Two stations were assembled and are optional. A third high-pressure station is being prepared.

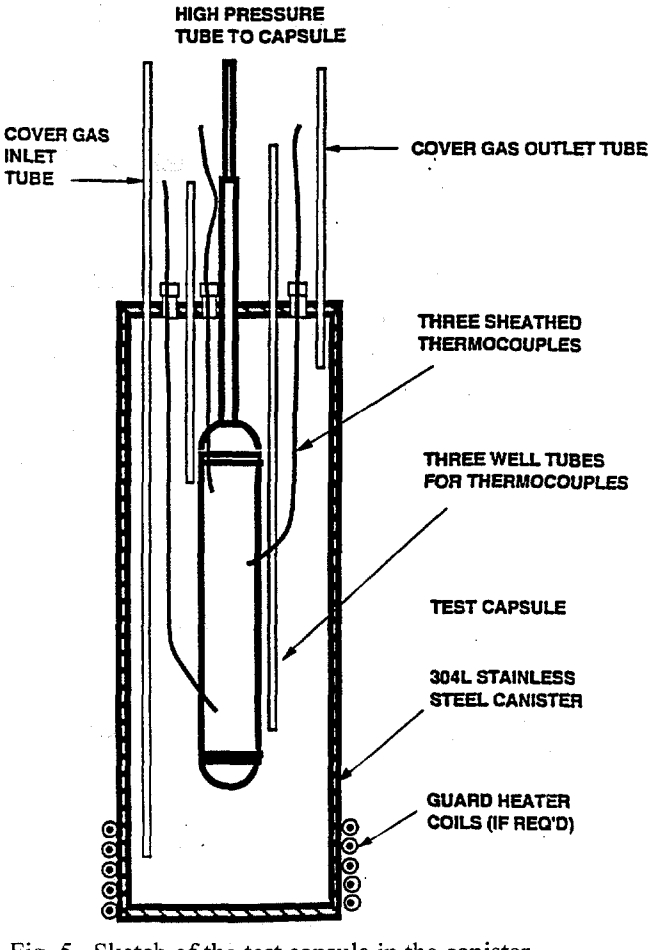

Fig. 5. Sketch of the test capsule in the canister.

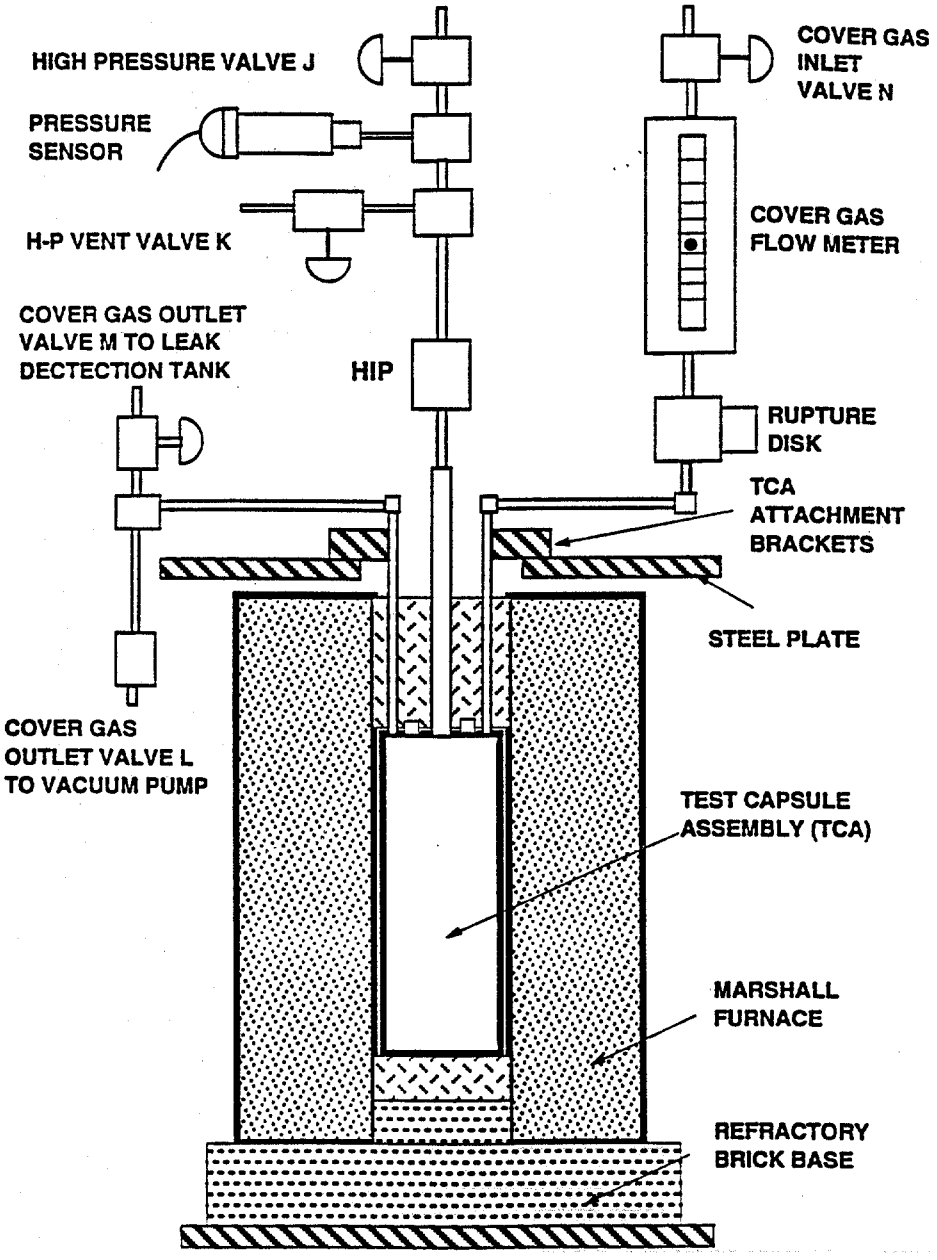

Fig. 6. Sketch of the pressurized capsule test station.

3.3.7 References

3. T. J. Dobry and S. T. Christenbury, *Advanced Long Term Battery Isotopic Heat Source Teat Plan,* Teledyne Energy Systems, Hunt Valley, MD, July 11, 2000.
4. R. W. Swindeman and R. L. Martin, *Advanced Long-Term Battery Heat Source Alloy Development and Characterization Year End Report,* Oak Ridge National Laboratory, Oak Ridge, TN (September 30, 1999).
5. R. W. Swindeman, *Review of the Mechanical Behavior of Haynes Alloy No. 25,* Oak Ridge National Laboratory, Oak Ridge, TN, July, 1998.
6. R. Widmer, et. al., *Mechanism Associated with Long Time Creep Phenomena,* Part 2, AFML-TR-65-181 (AD-815679) (March 1967).

3.4 B-SCAN AND ULTRASONICS

3.4.1 Background

In support of the Cassini mission to Saturn, ORNL and the Y-12 Plant were involved in the production of CVSs for use in radioisotope thermoelectric generators (RTG). As part of this effort, Y-12 developed a new ultrasonic inspection for the closure weld, based upon previous efforts used in the Galileo and Ulysses programs, but including new equipment and a new B-scan technique to identify benign problems such as WS fusion and weld mismatch. The basic inspection was documented by M. W. Moyer in "Ultrasonic Inspection of GPHS CVS Closure Welds," a report (Y/DW-1310) dated May 17, 1994. However, the B-scan technique was developed later but not fully documented. This effort is to produce a comprehensive report to document the full ultrasonic effort and show typical results from actual CVS welds.

3.4.2 Development of B-Scan Inspection

This report has been completed and is in the review process.

4.0 PLUTONIUM PRODUCTION STUDIES

4.1 TARGET DEVELOPMENT

4.1.1 Dosimeter Targets

The objective of the dosimeter target irradiations is to characterize ^{238}Pu production, especially ^{236}Pu content, at various locations in each reactor. Dosimeter targets were designed, fabricated, and inserted into both the INEEL/ATR and the ORNL/HFIR. The resulting data will provide a firm basis for selection of appropriate ^{237}Np (n,2n) ^{236}Pu and ^{237}Np (γ,n) ^{236}Pu cross section data sets.

It was previously reported that six dosimeter capsules, which had been irradiated in the ATR, were shipped to ORNL for isotopic analysis to determine ^{236}Pu content. However, the ATR dosimeter capsules had radiation doses larger than anticipated. Several modifications to the original post irradiation examinations were required in order to maintain low doses to workers. Results are expected in fall of 2000.

4.1.2 Target Pellet Tests

A conceptual design for a test pellet, developed in conjunction with INEEL/ATR, was discussed in the previous reporting period. A second conceptual design depicted in Fig. 1, has been developed for the ORNL/HFIR. The basic feature of the designs for target pellets is the use of an encapsulated mixture of Al and NpO_2 that has been compressed to ~80–90% of theoretical density in the form of a small pellet. These pellets are enclosed in an aluminum liner to ease the handling process while targets are fabricated. Once several pellets have been fabricated, they can be inserted into a target capsule and irradiated.

The pellets chosen for HFIR are slightly smaller than the ATR pellets to reduce the thermal load on the target. A pellet pressing test program was developed to examine various characteristics of the final pressed pellets. Methods for pellet powder blending, pellet pressing, and pellet QA were developed on cold mixtures of aluminum and cerium oxide for the smaller pellets. These methods were then applied to the NpO_2 pellet pressing.

Eight NpO_2 pellets were fabricated in glove boxes containing special pellet pressing equipment. NpO_2 was mixed with aluminum powder to fabricate pellets with 5, 10, and 20% by volume of NpO_2 and pressed to 80% and 90% of theoretical. The pellets were then radiographed and examined for defects and proper NpO_2 powder distribution. All pellets passed inspection and were loaded into six target tubes. Each target tube contained eight pellets: two each of the 5 vol.%-NpO_2 density pellets; two each of the 20 vol.%-NpO_2 density pellets, four each of the 10 vol.%-90% density pellets, and a dosimeter package. The targets were taken to HFIR and have been irradiated. Targets are scheduled for return to REDC in November, and chemical analysis will occur soon thereafter.

4.1.3 Waste Disposition

This effort begins with data from the FY 1999 studies and looks at technologies for waste minimization proposed in the early study. Of particular interest, is the desire to segregate waste in order to minimize TRU waste and allow treatment of selected waste streams. The solid waste is further subdivided into porous and nonporous waste. These waste streams will require different approaches to waste pretreatment and minimizing action.

We are currently investigating three methods of removing radioactive contamination from miscellaneous part sand equipment as a mechanism to eliminate a substantial portion of the non-porous radioactive waste. The three methods are (1) electrolytic decontamination, (2) chemical extraction with the TechXtract method, and (3) chemical oxidation with cerium (IV).

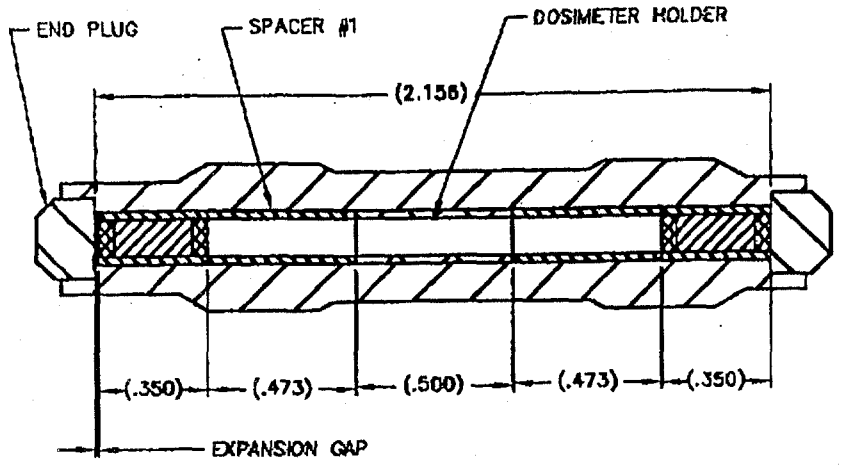

2–PELLET CONFIGURATION

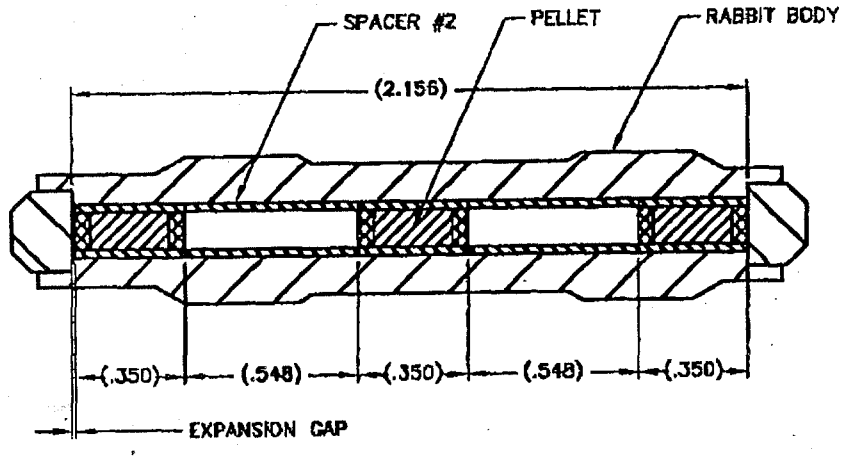

3–PELLET CONFIGURATION

Fig. 1. HFIR test rabbit assembly and loading diagram.

4.1.3.1 Electrolytic Decontamination

Electrolytic Decontamination

An electrolytic decontamination cell has been setup and testing with contaminated stainless steel plates was started. The plates are contaminated with a known quantity of ^{241}Am. Tests have been conducted at various temperatures and time intervals to determine the removal rate. Test results showed that electropolishing removes the contamination quite well; however, the removal rate is relatively slow.

Chemical Extraction with the TechXtract Method

Testing with the TechXtract chemicals and radioactive-contaminated plates was started. Initial test results show that the TechXtract process effectively removed the ^{241}Am tracer (>99% removal). The treatment process required a lot of handling and the solution was found to degrade over time. The TechXtract process was found to have several disadvantages as compared to the other processes tested.

Chemical Oxidation with Cerium (IV)

Testing with cerium (IV) nitrate and radioactive-contaminated tracer plates was started. Tests have been conducted by varying solution temperature and immersion times. The results show that the ^{241}Am was effectively removed from the plates (>99% removal). The effect of temperature on the decontamination was also tested. Overall, this use of Ce (+IV) was found to be the optimum method of decontamination.

Chemical Treatment with Nitric Acid

This treatment was added after seeing the success of the cerium (IV) nitrate. It was decided to determine how much of the contamination could be removed without the cerium (IV) component. Results showed that it may be reasonable to use the 0.5 M nitric acid as a first step to decontaminating items and then perhaps using one of the other treatment steps to further decontaminate the items.

4.2 CONCEPTUAL PLANNING

4.2.1 Conceptual Design Studies

Several related small studies supporting the conceptual design were carried out. The design philosophy as stated in the Preconceptual Design Report for the Plutonium Processing Facility (PPF) emphasizes utilizing equipment designs that were developed for Building 7920. Some of that equipment has components that are expensive or difficult to maintain. In some instances, equipment is over-designed for the radiation and chemical environments expected in the PPF. Additionally, there are differences between the two facilities and differences in the operations which will require new designs of selected items. Finally, there will be an increased emphasis on procurement of off-the-shelf components in order to reduce costs and/or future maintenance requirements. Many of the items found on equipment racks are unique and may require longer lead time to design than standard industrial components. It is primarily these such things that this early design effort examined.

A focus of this study was on equipment which will be located inside the hot cells or which will interface directly with such equipment. Some of the equipment will be located on equipment racks which are stainless steel structures on which small pieces of processing equipment such as valves and pumps are located. The racks also contain the interconnecting piping and have a unique method for connecting to external services and other equipment racks. Equipment racks have been used successfully at the REDC for over thirty years. The in-cell equipment must be designed for the hot cell radiation and chemical environment and must be capable of being operated and replaced or

repaired using remote handling techniques. Ideally repairs would be able to be performed without removing the item from the hot cell.

This study also examined parts of the existing ventilation and liquid waste handling systems to determine their suitability for use as is.

The report focused on valves used in cell to control liquid flow, replaceable in-cell HEPA filters, the off-gas scrubber used for removing acid fumes from the cell ventilation, and replaceable piping bundles for bringing fluids into equipment racks.

The air operators for valves were identified as potential substitutes. These were purchased at the end of the reporting period. Concepts for the design interfaces with the valve, valve operator, and equipment rack will need to be developed.

Many types of gas scrubbers were identified for use in the proposed ventilation system. Croll-Reynolds and Schutte & Koerting were contacted to obtain information on the venturi-type scrubbers which they manufacture. Another company, AEA Technology, makes an operationally-similar unit called a V-tex scrubber. An advantage of working with AEA Technology is that they are familiar with the design of equipment for remote operations. There are many types of gas scrubbers and the best type for this application needs to be determined. Croll-Reynolds and Schutte & Koerting were contacted to obtain information on the venturi-type scrubbers which they manufacture. Another company, AEA Technology, makes an operationally-similar unit called a V-tex scrubber. An advantage of working with AEA Technology is that they are familiar with the design of equipment for remote operations. Further effort will be needed to determine the optimal scrubber system.

Conceptual designs of piping bundles were prepared. The piping bundles have been designed to be replaceable.

Several concepts for in-cell HEPA filtration were examined with the intent of finding a unit that would be readily replaceable using remote handling systems. Sketches for units were developed and presented in the report. Concepts for replacement were also developed and presented.

INTERNAL DISTRIBUTION

1. E. P. George
2. J. S. Ivey
3. J. F. King
4. C. G. McKamey
5-7. J. P. Moore
8. E. K. Ohriner
9. G. R. Romanoski
10. G. B. Ulrich
11. M. C. Vance
12. R. M. Wham
13. Laboratory Records

EXTERNAL DISTRIBUTION

14-23. U. S. DEPARTMENT OF ENERGY, NE-50, Germantown Building, 11901 Germantown Road, Germantown, MD 20874-1290

C. E. Brown
J. Dowicki
L. W. Edgerly
R. R. Furlong
L. C. Herrera
A. S. Mehner
W. D. Owings
R. C. Raczynski
L. L. Rutger
E. J. Wahlquist

24. DEPARTMENT OF ENERGY, Albuquerque Field Office, P.O. Box 5400, Albuquerque, NM 87115

R. L. Holton

25-26. DEPARTMENT OF ENERGY, Oak Ridge Operations Office, Bldg. 4500N, Oak Ridge, TN 37831

L. W. Boyd, Mail Stop 6390
S. R. Martin, Jr., Mail Stop 6269

27. DEPARTMENT OF ENERGY, Los Alamos Area Office, 528 35th Street, Los Alamos, NM 87544

R. J. Valdez

28. DEPARTMENT OF ENERGY, Savannah River Operations Office, Bldg. 703F, P.O. Box A, Aiken, SC 29802

S. W. McAlhaney

29. DEPARTMENT OF ENERGY, Miamisburg Office, P.O. Box 66, Miamisburg, OH 45342

T. A. Frazier

30-31. BABCOCK AND WILCOX OF OHIO, INC., 1 Mound Road, Miamisburg, OH 45343-3000

D. M. Gabriel
J. R. McDougal

32-33. LOCKHEED MARTIN ASTRONAUTICS, P.O. Box 8555, Philadelphia, PA 19101

R. J. Hemler
R. M. Reinstrom

34. LOS ALAMOS NATIONAL LABORATORY, P.O. Box 1663, NMT-9, MS E502, Los Alamos, NM 87545

E. M. Foltyn

35. TETRA TECH NUS INC., 910 Clopper Road, Suite 400 Gaithersburg, MD 20878-1399

B. W. Bartram

36-37. ORBITAL SCIENCES CORPORATION, INC., 20301 Century Blvd., Germantown, MD 20874

R. T. Carpenter
E. A. Skrabek

38. PHILLIPS LABORATORY, Kirtland Air Force Base, AFRL/VSDV, 3550 Aberdeen Avenue SE, NM 87117

C. Mayberry

39. TELEDYNE BROWN ENGINEERING-ENERGY SYSTEMS, 10707 Gilroy Road, Hunt Valley, MD 21031

M. F. McKittrick

40. TEXAS A&M UNIVERSITY, Center for Space Power, Mail Stop 3118, College Station, TX 77843

M. J. Schuller

41. WESTINGHOUSE ADVANCED TECHNOLOGY BUSINESS AREA, P.O. Box 355, Pittsburgh, PA 15230-0355

M. O. Smith

42. WESTINGHOUSE SAVANNAH RIVER COMPANY, Savannah River Site, Aiken, SC 29808

R. W. Saylor